

## Diffusion of Ca and Mg in calcite

DIANA K. FISLER\* AND RANDALL T. CYGAN†

Geochemistry Department, Sandia National Laboratories, Albuquerque, New Mexico 87185-0750, U.S.A.

### ABSTRACT

The self-diffusion of Ca and the tracer diffusion of Mg in calcite have been measured experimentally using isotopic tracers of  $^{25}\text{Mg}$  and  $^{44}\text{Ca}$ . Natural single crystals of calcite were coated with a thermally sputtered oxide thin film and then annealed in a  $\text{CO}_2$  gas at 1 atm total pressure and temperatures from 550 to 800 °C. Diffusion coefficient values were derived from the depth profiles obtained by ion microprobe analysis. The resultant activation energies for Mg tracer diffusion and Ca self-diffusion are, respectively:  $E_a(\text{Mg}) = 284 \pm 74$  kJ/mol and  $E_a(\text{Ca}) = 271 \pm 80$  kJ/mol. For the temperature ranges in these experiments, the diffusion of Mg is faster than Ca. The results are generally consistent in magnitude with divalent cation diffusion rates obtained in previous studies, and provide a means of interpreting the thermal histories of carbonate minerals, the mechanism of dolomitization, and other diffusion-controlled processes. The results indicate that cation diffusion in calcite is relatively slow and cations are the rate-limiting diffusing species for the deformation of calcite and carbonate rocks. Application of the calcite-dolomite geothermometer to metamorphic assemblages will be constrained by cation diffusion and cooling rates. The direct measurement of Mg tracer diffusion in calcite indicates that dolomitization is unlikely to be accomplished by Mg diffusion in the solid state but by a recrystallization process.

### INTRODUCTION

The experimental evaluation of chemical diffusion in minerals provides the geochemist with diffusion coefficients required for the interpretation of numerous transport-controlled processes including creep, chemical alteration, homogenization, and dissolution. Although significant on geologic time scales, the effect of typical solid-state diffusion in mineral lattices for laboratory time scales is very slow. Consequently, it has been very difficult for experimentalists to obtain precise and accurate measurements of diffusion coefficients. Some of the solutions to this experimental difficulty include performing the diffusion anneals at elevated temperatures to accelerate the diffusion (e.g., Elphick et al. 1985) or observing the influence of diffusion on more macroscopic features such as the homogenization of very fine exsolution lamellae (e.g., Brady and McCallister 1983). To apply these alternative laboratory measurements to geologic conditions involves extrapolating diffusion rates measured at very high temperatures by several hundred degrees. Such extrapolations are only valid if the diffusion mechanism remains the same across a wide temperature range and if the activation energy was determined with enough precision. Therefore, it is important that the measurement of diffusion rates in minerals be performed at the temperature of interest for the application, or at least at temperatures as close as possible to that temperature. Furthermore, it is de-

sirable to create a framework for fully understanding the fundamental mechanisms for diffusion (i.e., the defect structure of a mineral) so that laboratory results may be applied confidently to natural processes. The most direct experimental method for determining chemical and self-diffusion rates involves the use of various analytical techniques to determine the transport of isotopic tracers in the mineral lattice. Analytical techniques having high spatial resolution, such as ion microprobe analysis and Rutherford backscattering, have provided a means of reexamining previously intractable problems related to diffusion in minerals (e.g., Schwandt et al. 1998; Cherniak 1997, 1998).

Carbonate minerals are a major constituent of sedimentary and some metamorphic rocks. The most common carbonate mineral in terrestrial sediments is calcite ( $\text{CaCO}_3$ ). Calcite and other carbonate phases typically incorporate a number of minor and trace elements and preserve cation assemblages that routinely violate the stabilities predicted by phase equilibria (Reeder and Grams 1987). As such, carbonate phases may preserve information about the chemical and thermodynamic environment in which they originated and processes by which they formed. The dolomitization of limestone is one example of a diagenetic processes that is poorly understood (e.g., Hardie 1987). Many of the previous investigations of carbonate mineral geochemistry have focused on the interaction of fluids with the carbonate surface (dissolution and precipitation processes) because carbonate minerals are rarely found “dry” on Earth. However, when carbonate globules were identified in a meteorite of Martian origin (Romanek et al. 1994), the debate over the thermal history of the parent rock dramatically illustrated the necessity for fundamental measurements of intrinsic prop-

\*Present address: Johns Manville Technical Center, 10100 W. Ute Avenue, P.O. Box 625005, Littleton, Colorado 80121, U.S.A.

†E-mail: rtcygan@sandia.gov

erties of carbonate minerals. Studies of cation diffusion in carbonate phases are restricted to relatively low-temperature measurements, because the carbonate phases readily decompose to  $\text{CO}_2$  and the oxide component. Sensitive analytical methods therefore can be used to determine the limited diffusion distances of tracer species in the mineral.

Previous studies of chemical diffusion in calcite include the measurement of carbon and oxygen rates by Anderson (1969) and by Haul and Stein (1955). Both of these studies utilized an indirect method of determining the diffusion coefficients in which carbon dioxide is bulk-exchanged with calcite powder. More recently, Kronenberg et al. (1984) used an ion microprobe and isotopic tracers to measure carbon and oxygen diffusion rates between 500 and 800 °C. They determined that, despite the anisotropic crystal structure (rhombohedral) of calcite, there was negligible orientation dependence for carbon or oxygen diffusion and carbon diffusion rates strongly depended on Mn concentration and water pressure. Until recently, the only constraint on cation diffusion in calcite was the estimate of the upper limit at 800 °C determined experimentally by Bratter et al. (1972). However, Farver and Yund (1996), in a study emphasizing grain boundary diffusion in calcite aggregates, also measured volume self-diffusion in calcite from 700–900 °C and found no orientation dependence. Recently, Cherniak (1997, 1998) determined diffusion coefficients for a number of trace and rare earth elements in carbonates using Rutherford backscattering at temperatures from 400–800 °C.

Beyond the difficulties encountered with the analysis of the diffusion profiles is the limitation imposed by the decomposition and transformations of carbonate phases at elevated temperatures; several reversible phase transitions associated with calcium carbonate occur at high temperatures. Mirwald (1976) performed differential thermal analysis (DTA) experiments at high pressures, which suggest a phase transition from  $\text{CaCO}_3(\text{I})$  to  $\text{CaCO}_3(\text{IV})$  at temperatures from 720 to 780 °C at 8 and 18 kbar, respectively. Extrapolation of this transition point to 1 atm pressure suggests a transition temperature of ~810 °C. A later study of this phase transition by Mirwald (1979a) at 1 bar  $\text{CO}_2$  pressure confirms the phase transition at 800 °C. In addition, electrical measurements by Mirwald (1979b) show changes in the activation energy of electrical conductivity at 40 bars  $\text{CO}_2$  pressure at 500, 725, 800, and 985 °C. The two higher temperatures changes have been interpreted as an onset of rotational disorder at 725 °C and a change to the  $\text{CaCO}_3(\text{IV})$  phase at 800 °C.

In the present study, tracers of Mg and Ca were used to determine the cation diffusion rates in calcite over the temperature range from 550 to 800 °C. This work is intended to provide the critical data on the diffusion of major elements in calcite and will necessarily complement the recent experimental studies by Cherniak (1997, 1998) on the diffusion of trace elements in calcite. The experimental approach relies on the use of thin films to create the diffusion couple and an ion microprobe to analyze the resulting depth profiles.

## EXPERIMENTAL PROCEDURE

The experimental procedure used in the present study to examine cation diffusion in calcite was developed originally by

Schwandt et al. (1993) for measuring cation diffusion rates in mantle phases. The thin-film technique involves two significant improvements over earlier diffusion measurements that utilized diffusion couples. The first improvement is the use of the ion microprobe, which has excellent depth resolution and is capable of obtaining depth profiles of both major and trace element components and isotopic tracer species. The second improvement is the use of a vacuum sputtering technique for the deposition of a thin film onto the mineral substrate. Schwandt et al. (1993) demonstrated the successful use of thermal sputtering in a vacuum chamber to provide a thin and extremely flat coating of an isotopically enriched oxide of the tracer species. The vacuum sputtering excludes moisture during the deposition process; water, or more specifically the activity of  $\text{H}_2\text{O}$ , has been shown to enhance the diffusion of oxygen in calcite (Kronenberg et al. 1984; Farver and Yund 1996).

Samples of optically clear single crystal calcite from Chihuahua, Mexico, were obtained through local mineral shops. Electron microprobe analysis of the samples for (over 200 sampling points) showed that they have a composition equal to stoichiometric  $\text{CaCO}_3$  with 0.25 wt%  $\text{MgO}$ , 0.02 wt%  $\text{MnO}$ , and 0.02 wt%  $\text{FeO}$ , but no detectable  $\text{SrO}$ . The calcite surfaces were examined optically, and the most uniform cleavage surfaces were selected for vacuum coating with isotopic tracers of Mg and Ca. In two cases, the surfaces were polished using progressively finer grits of diamond pastes, ending with a 0.05  $\mu\text{m}$  silica slurry. Diffusion coefficients obtained from these samples were compared with those results obtained using the cleaved surfaces. However, the majority of the experimental determinations were performed on cleaved surfaces to avoid mechanical surface damage due to polishing. No pre-annealing of the samples was performed. Because of the lack of anisotropic diffusion behavior observed by Kronenberg et al. (1984) and Farver and Yund (1996), the present study only examined diffusion perpendicular to the (104) cleavage surface.

A thin film (~1000 Å) coating of an isotopically enriched oxide was deposited in a high-vacuum chamber onto the cleaved or polished (104) surface of the calcite samples by resistively heating a W crucible containing either  $\text{MgO}$  enriched 98.8% in the  $^{25}\text{Mg}$  isotope or  $\text{CaO}$  enriched 98.5% in the  $^{44}\text{Ca}$  isotope. The vacuum chamber was back-filled with 10%  $\text{O}_2$  gas for depositing the coatings involving Mg. In a previous study of Mg diffusion in enstatite (Fisler, unpublished manuscript), transmission electron microscopy of similarly prepared enstatite-oxide diffusion couples indicated that the high temperatures necessary to evaporate  $\text{MgO}$  also evaporates some W metal onto the mineral surface. However, the W did not influence the exchange and diffusion of the Mg between phases.

The calcite-oxide diffusion couples were annealed in 1 atm of flowing  $\text{CO}_2$  for ~12–4000 hours at temperatures ranging from 550 to 800 °C in a vertical Deltech furnace. The quenched samples were then analyzed using a Cameca IMS 4f ion microprobe operating at 10 or 12.5 kV using a 100 nA  $\text{O}^-$  beam, ~45  $\mu\text{m}$  spot size, and 80% of a 250  $\mu\text{m}$  × 250  $\mu\text{m}$  raster area. In a few cases, depth profiles were obtained using beam currents of 50 nA and 200 nA for comparison. Intensities for each mass (or isotope) were counted for a duration of 10 s before cycling to the next mass. The long-duration experiments have

an uncertainty in the reported time of up to 0.5% due to occasional power outages, although no more than one power outage occurred for any one diffusion anneal. The uncertainty in the reported temperatures is  $\pm 2$  °C.

To obtain the proper diffusion depth profiles (concentration vs. distance) it is necessary to convert the time axis of Figures 2 and 3 (or number of analytical cycles of Fig. 1) to distance based on the depth into the sample that the primary beam of the ion microprobe has analyzed. In this effort, the depth of penetration for an uncoated calcite sample subjected to the sputtering of the ion beam was measured using a contact profilometer. The sputtering rate was derived from the depth of the crater profile vs. the sputtering time. Several different calcite samples were used for the calibration that was rechecked on each analysis day.

Diffusion experiments were performed at 575 and 600 °C for different anneal durations to ensure that the resulting diffusion coefficients were invariant with respect to time. A zero time experiment, in which the diffusion couple was brought up to the experimental conditions then immediately quenched, did not show evidence of any diffusion in either of the Ca or Mg experiments.

## RESULTS

After removal from the furnace, diffusion samples were examined visually and optically for evidence of changes or instability. Experimental results reported here were obtained for conditions below the temperature at which  $\text{CaCO}_3$  decomposes, as determined by Goldsmith (1959). For example, at 800 °C, one experiment failed when the  $\text{CO}_2$  gas source was exhausted during the course of the anneal. The sample was removed from the furnace within a few hours; however, obvious frosting of the sample was visible, presumably due to calcite decomposition. Furthermore, there was clear optical evidence (frosting) of decomposition along the cleavage planes. One diffusion experiment was attempted at 900 °C resulting in a sample that had clearly decomposed. All successful analyses presented herein were performed on samples that were visually and optically identical to their pre-annealed condition. Typical ion depth profiles are shown in the Figures 1 (for Ca self-diffusion) and 2 (for Mg tracer diffusion). Analysis of the samples for the Ca self-diffusion experiments involved the monitoring of masses corresponding to  $^{44}\text{Ca}$ ,  $^{40}\text{Ca}$ ,  $^{42}\text{Ca}$ ,  $^{25}\text{Mg}$ ,  $^{55}\text{Mn}$ , and  $^{54}\text{Fe}$ . Mg tracer diffusion rates were derived from the analysis of  $^{40}\text{Ca}$ ,  $^{42}\text{Ca}$ ,  $^{25}\text{Mg}$ ,  $^{55}\text{Mn}$ , and  $^{54}\text{Fe}$ .  $^{12}\text{C}$  was also monitored during the depth profile analysis of several samples to indicate the presence of calcite and determine the position of the diffusion-couple interface.

Figure 1 displays the high concentration of the isotopic tracer  $^{44}\text{Ca}$  at the diffusion couple surface for a Ca diffusion experiment completed at 600 °C. Mass intensity is presented as a function of the analytical cycle as the primary beam etches further into the sample. There is an increase in the natural  $^{40}\text{Ca}$  intensity to indicate the position of the oxide-calcite interface and subsurface. Figure 2 shows a depth profile of calcite with the  $^{25}\text{MgO}$  coating after being annealed at 700 °C. The depth profile, presented here as a function of analysis time, illustrates the diffusional penetration of the Mg tracer into the calcite and

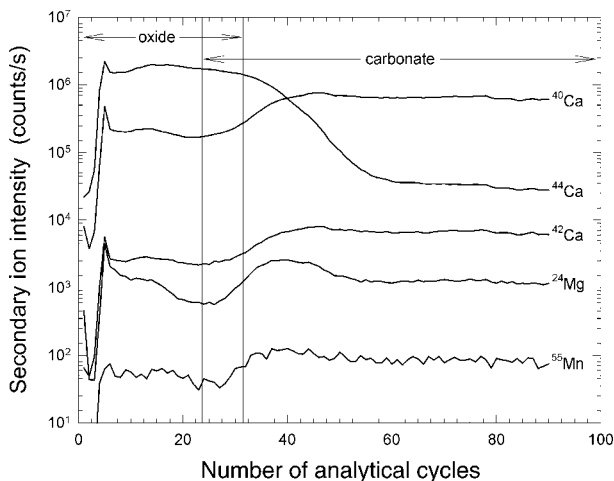


**FIGURE 1.** Ion microprobe depth profiles for Ca diffusion in calcite as a function of analysis cycle for sample cc600a annealed at 600 °C showing the concentration of  $^{24}\text{Mg}$ ,  $^{40}\text{Ca}$ ,  $^{42}\text{Ca}$ ,  $^{44}\text{Ca}$ ,  $^{55}\text{Mn}$ , and the limits on the inferred position of the interface between the thin film coating and the calcite substrate (modified from Fisler and Cygan 1998).

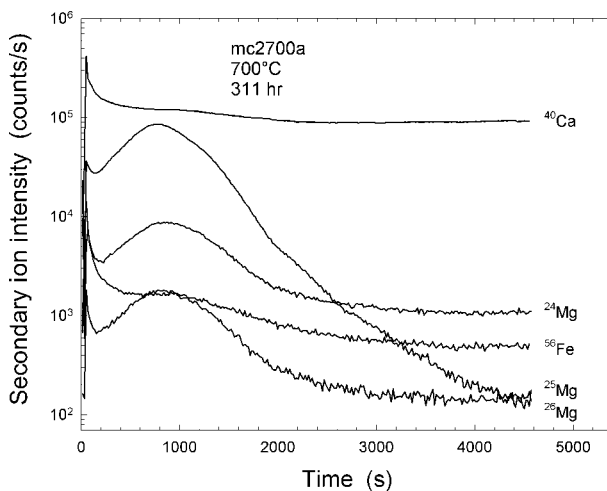


**FIGURE 2.** Depth profiles for Mg tracer diffusion in calcite as a function of analysis time for sample mc2700a annealed at 700 °C. Note the significant decrease of the  $^{25}\text{Mg}$  intensity relative to the apparently constant  $^{40}\text{Ca}$  intensity resulting from the use of a log scale for the mass intensity.

the variation of concentrations before reaching the bulk composition of the calcite. Calcium is present throughout the surface layer. In several other ion microprobe analyses, the concentration of carbon was also monitored. Figure 3 includes a depth profile for an Mg tracer experiment demonstrating a significant concentration of Ca in the surface layer accompanied by a lower than expected  $^{12}\text{C}$  for the bulk region of the carbonate. The surface layer probably represents a mixed oxide layer that includes a high concentration of Ca resulting from the exchange of Ca for Mg from the calcite. The transport of Ca provides the counter-flux necessary for Mg to diffuse into

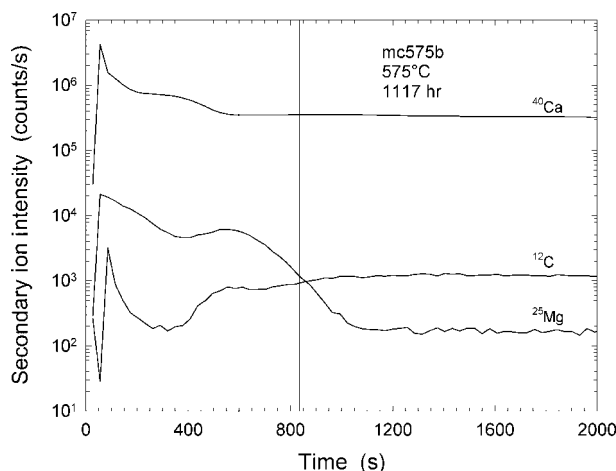


**FIGURE 3.** Selected mass depth profiles for Mg tracer diffusion in calcite as a function of analysis time for sample mc575b annealed at 575 °C. The plot illustrates the decrease in  $^{25}\text{Mg}$  content within the bulk calcite and the inferred location of the interface between the surface oxide layer and the calcite substrate.

the carbonate. At longer times (greater depth), there is an increase in the intensity of  $^{12}\text{C}$  indicating the onset of the primary beam sputtering into the carbonate phase. The C content at this position is slightly lower than that observed for analyses of the bulk calcite. This result is observed consistently for those analyses in which C was monitored (as  $^{12}\text{C}$ ) and may be related to the formation of molecular C species during analysis through the oxide film.

An average sputtering rate of  $3.3 \pm 0.2 \text{ \AA/s}$  (at 100 nA) for the calcite was obtained and used to convert the analyses to depth profiles. The surface oxide layer was subtracted from the depth profile once the location of the diffusion couple interface was identified and noted as time zero. In previous diffusion studies using this technique, the location of the interface had been determined by obvious discontinuities in the ratio of minor elements to major elements (e.g., Schwandt et al. 1998). In the present set of experiments, such sharp discontinuities were rarely observed. We have chosen the position of the interface between the mineral and the oxide coating by a number of qualitative factors, including the initial point of increase of the  $^{12}\text{C}$  signal relative to the bulk calcite composition and the occurrence of the maximum isotopic tracer concentration. Because the diffusion coefficient obtained using an error function model depends on the curvature of the concentration profile, identification of the precise position of the interface is not crucial. However, the more data utilized from the concentration profile, especially from the curved section, the more statistically accurate the least-squares fit will be. The results presented here are based on the use of the maximum isotopic composition as a consistent choice for the diffusion couple interface and the beginning of the diffusion profile.

An example of a depth profile for Ca self-diffusion at 650 °C is presented in Figure 4. The concentration is presented as a ratio of the intensity of the tracer isotope  $^{44}\text{Ca}$  to the intensity of the naturally abundant isotope  $^{40}\text{Ca}$ , which helps to remove the effect of small fluctuations in beam current that occasionally

occur during the analyses. Typically, the depth of penetration for the enriched Ca isotope is a few tenths of micrometers, whereas in the Mg tracer diffusion experiments the depth of penetration of Mg into calcite ranged from a few tenths to several micrometers. This difference is primarily related to the greater temperature range used for the Mg experiments but also is associated with the differences in the diffusion energetics and the ionic radii of the cations. A series of very low temperature (500 and 525 °C) diffusion experiments were attempted; however, the extremely short diffusion profiles (less than 0.05  $\mu\text{m}$ ), combined with the need to sputter through an equivalently sized surface layer, rendered the analysis of the profiles questionable and did not provide an unambiguous value for the diffusion coefficient.

For the Mg diffusion experiments, several diffusion anneals were performed at a given temperature but for varying times of anneal (Table 1). The resulting diffusion coefficients are in statistical agreement within the calculated uncertainty for the individual samples. Although longer durations for the time series experiments were impractical for this study, the results suggest a diffusional invariance with time. The longer anneal times required for the lowest temperature samples did not allow such an independent check of the time independence and uncertainty of the results.

Several attempts to measure the Mg tracer diffusion rates in other carbonate minerals, including rhodochrosite, magnesite, and dolomite, were unsuccessful. Instability of the phases at temperatures high enough to induce sufficient diffusive transport of the cations at 1 bar of  $\text{CO}_2$  pressure prevented such measurements. Diffusion couples with rhodochrosite and magnesite showed marked discoloration even at very short anneal times (< 10 h), and the dolomite fragmented violently at very low temperatures even while using a slow temperature ramp and with elevated  $\text{CO}_2$  pressures. Microscopic examination of

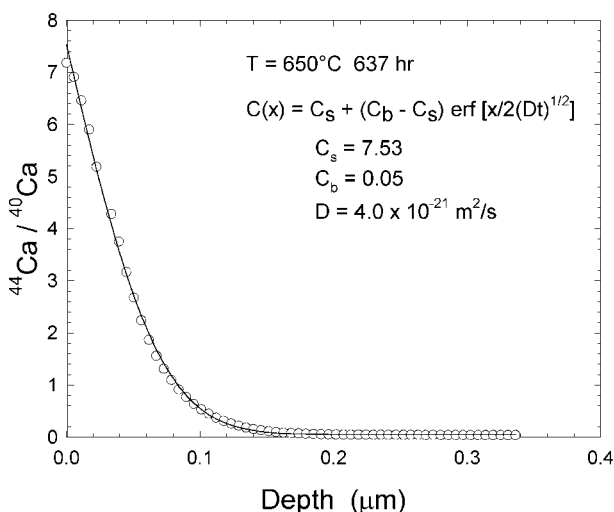


**FIGURE 4.** Intensity ratio of  $^{44}\text{Ca}$  to  $^{40}\text{Ca}$  in calcite as a function of calcite depth for sample cc650b annealed at 650 °C. The best fit (line) of an error function diffusion model to the experimental data (circles) is provided.

**TABLE 1.** Experimental conditions and resulting diffusion coefficients

Sample and run no.	Temperature (°C)	log $D_{Ca}$ (m <sup>2</sup> /s)	log $D_{Mg}$ (m <sup>2</sup> /s)	Duration of experiment (h)
cc650a	650	-20.61		637
cc650b	650	-20.32		637
cc600a	600	-21.70		912
cc600b	600	-21.46		912
cal-1 (polished)	600	-21.72		1272
cal-2 (polished)	600	-21.63		1272
cc550a	550	-22.36		4314
cc550b	550	-22.30		4314
mc800a	800		-16.90	12
mc800b	800		-17.20	12
mc750a	750		-17.90	86
mc750b	750		-18.40	86
mc1700a	700		-18.90	142
mc1700b	700		-19.10	142
mc2700a (200 nA)	700		-19.29	311
mc2700b (200 nA)	700		-19.01	311
mc600a	600		-20.78	736
mc600b	600		-20.49	736
mc2600a	600		-20.26	1001
mc2600b	600		-20.31	1001
mgca575a	575		-21.17	736
mgca575b	575		-21.23	1117
mgca575c	575		-21.21	1117
mgca550a	550		-21.40	3943
mgca550b	550		-21.40	3943

Notes: All diffusion anneals performed at 1 atm CO<sub>2</sub> on cleaved (104) surfaces, except where noted. All analyses reported were performed at a 100 nA beam current, except where noted.

the magnesite showed a pervasive cracking pattern on the mineral surface after the high-temperature anneals. Depth profiles obtained for the annealed magnesite sample showed a <sup>25</sup>Mg/<sup>12</sup>C ratio that is consistent with the unannealed magnesite, indicating that decomposition of the sample to MgO + CO<sub>2</sub> was avoided. However, the cracking of the surface is likely to have introduced fast transport paths for the enriched isotope. Future experiments might circumvent the instability problems by performing the diffusion anneals at high pressure using cold-seal vessels and a CO<sub>2</sub> pressure medium.

The diffusion profiles of isotopic ratio vs. distance were fit to a semi-infinite diffusion model (Crank 1975). Some previous investigators (Farver and Yund 1994; Ganguly et al. (1998) have linearized the model using an inverse error function while keeping the surface and bulk concentrations fixed and only allowing the diffusion coefficient to be varied during the fit to the experimental data. In contrast, it is possible to improve the fit of the diffusion model by also allowing the bulk and surface concentrations to vary using a numerical least-squares fitting algorithm. This latter method was used to obtain the diffusion coefficient values based on the best fit to the <sup>44</sup>Ca/<sup>40</sup>Ca and the <sup>25</sup>Mg/<sup>40</sup>Ca diffusion profiles as described by the error function diffusion model:

$$C_x = C_s + (C_b - C_s) \operatorname{erf} [x/2(Dt)^{1/2}] \quad (1)$$

$C_x$  is the concentration at depth of penetration  $x$ ,  $C_s$  is the concentration at the surface,  $C_b$  is the bulk concentration,  $t$  is the duration of the anneal, and  $D$  is the diffusion coefficient for either the Ca or Mg tracer isotope.

Equation 1 was fit to the experimental diffusion profiles using a linear least-squares fitting method while allowing  $C_s$ ,  $C_b$ , and  $D$  to vary, with the concentration represented by the

isotopic ratio. Experience in performing the curve fits and manipulation of the data indicated that the concentration in the bulk of the calcite,  $C_b$ , is not expected to vary significantly and that the exact identification of the interface position ( $x = 0$ ) is not crucial to the quality of the fit to the model. Curve fits were obtained using different choices of the interface position resulting in the same diffusion coefficient value within error of the measurement. The concentration in the bulk of the calcite was observed to be in agreement with the expected natural abundances for the Ca isotope ratio, Mg isotope ratio, and total Mg content.

A summary of the experimental conditions and diffusion coefficients is presented in Table 1. Uncertainties associated with the fit of the diffusion model are smaller than the experimental error derived from repeated analyses of depth profiles on the same sample. Experimental errors are primarily due to deviations in the ion microprobe beam current and spot size, yielding slight variations in sputtering rate and unevenness of the surface and interface. The cumulative error associated with the diffusion measurements is presented graphically in Figure 5.

Table 1 shows that there is no statistical difference between the diffusion coefficients obtained for the cleaved and polished calcite surfaces compared to those values determined for the simply cleaved surfaces. The two polished samples used for the determination of Ca self-diffusion coefficients at 600 °C agree with those derived for the unpolished samples. In contrast to the studies of diffusion in silicate minerals (e.g., Ryerson et al. 1989), it appears that calcite does not require a pre-anneal treatment to avoid this type of mechanical damage on a cleavage surface.

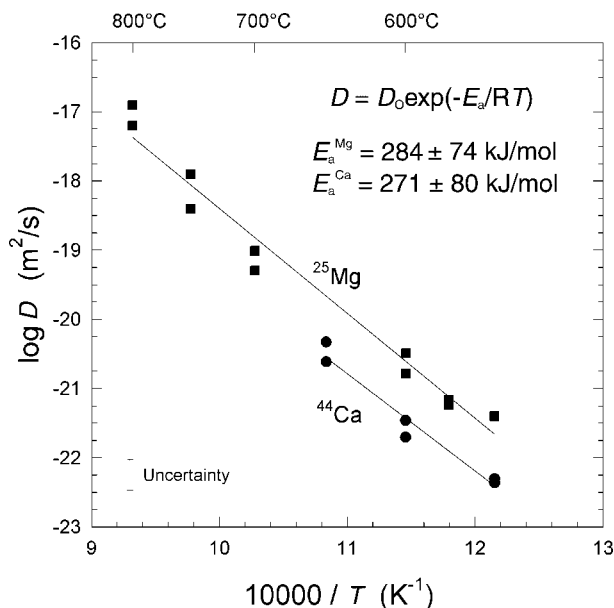


**FIGURE 5.** Arrhenius plot for Ca self-diffusion and Mg tracer diffusion in calcite. The error bar shown in the lower left represents the cumulative uncertainty in the final measurement based on the propagation of errors associated with the curve fitting and profile-to-profile variation.

Figure 5 provides an Arrhenius plot summarizing the Ca self-diffusion and Mg tracer diffusion data in calcite as derived from the above analysis of the experimental depth profiles. Note that the diffusion coefficients derived from duplicate experiments and analyses are presented for each temperature and fall within the experimental uncertainty. The activation energies are derived from the best fit of the Arrhenius relation to the data:

$$D = D_0 \exp(-E_a/RT) \quad (2)$$

where  $D_0$  is the pre-exponential parameter,  $E_a$  is the activation energy,  $R$  is the gas constant, and  $T$  is the absolute temperature.

## DISCUSSION

The diffusion rates for Ca self-diffusion and Mg tracer diffusion follow an Arrhenius relationship over the range of temperatures studied and show no effect due to the phase transitions indicated by DTA or electrical conductivity (Mirwald 1976, 1979b). Linear-least squares fits of Equation 2 to the data in Figure 5 yield the following values:  $\log D_0 = -5.3 \text{ m}^2/\text{s}$  and  $E_a = 271 \pm 80 \text{ kJ/mol}$  for Ca self-diffusion in calcite;  $\log D_0 = -3.26 \text{ m}^2/\text{s}$  and  $E_a = 284 \pm 74 \text{ kJ/mol}$  for Mg tracer diffusion in calcite. Magnesium diffusion rates are faster than those for Ca and are not unexpected because of the much smaller ionic radius for Mg (0.66 Å) relative to that for Ca (0.99 Å). Additionally, the tracer diffusion results are intrinsically faster for Mg because of the chemical potential driving force associated with Mg in calcite (i.e.,  $\text{Ca}_{1-x}\text{Mg}_x\text{CO}_3$ ) in comparison with the self-diffusion of Ca in calcite (i.e.,  $x = 0$ , pure  $\text{CaCO}_3$ ). The experimental activation energies are very similar for both Mg and Ca, and suggest that both these divalent cations migrate by a similar diffusion path and process.

Figure 6 compares the experimental diffusion rates and activation energies to those obtained by Cherniak (1997, 1998) for the divalent cations Sr and Pb, by Farver and Yund (1996) for Ca, and by Kronenberg et al. (1984) for C. All the divalent cations are expected to occupy similar sites in the calcite structure. The low activation energy (132 kJ/mol) that was obtained by Cherniak (1997) for Sr diffusion in calcite is in marked contrast to the Ca results of this study and that of Farver and Yund (1996). Strontium, which is known to occupy the Ca sites in calcite, is most likely transported by an alternate diffusion mechanism involving interstitial sites, in contrast to the mechanism for Ca transport that most likely involves Ca vacancies. The electrical conductivity and electromotive measurements of Mirwald (1979b) indicate that charge transport is accomplished by the motion of negatively charged defects. This results, combined with the covalency of the  $\text{CO}_3^{2-}$  group, suggest that Ca vacancies are the dominant defect in calcite and, therefore, probably control the mechanism for the diffusional transport of Ca ions.

A notable characteristic of the Arrhenius results presented in Figure 6 is the discrepancy between the data for self-diffusion of Ca in calcite reported by Farver and Yund (1996) and the values from this study. However, taking into account the associated errors in the reported activation energies, there is remarkably good agreement between the two different Ca data sets. The high-temperature conditions of Farver and Yund (1996), especially at 900 °C, suggest that the calcite would be unstable and would lead to a spurious activation energy; how-

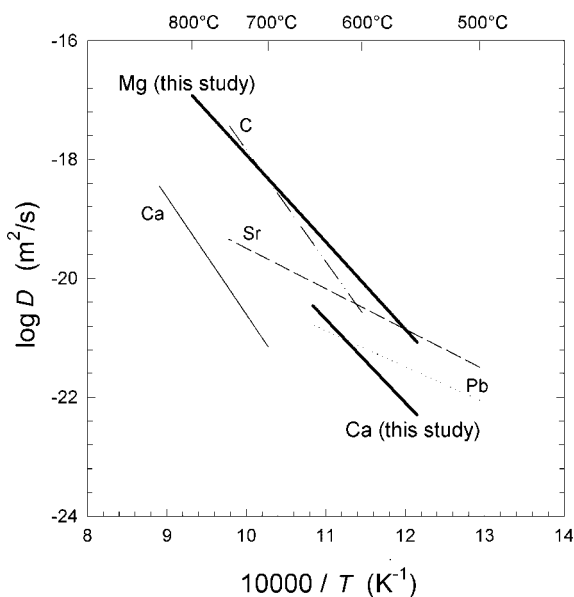


**FIGURE 6.** Summary Arrhenius plot of diffusion coefficients for (Mg, Ca) this study compared to previous studies of cation and carbon diffusion in calcite. Calcium self-diffusion from Farver and Yund (1996) designated by Ca; strontium (Sr) and lead (Pb) tracer diffusion rates from Cherniak (1997; 1998); carbon diffusion rates from Kronenberg et al. (1984).

ever, these investigators observed no evidence for decomposition in any of their samples (Farver, personal communication). Even if the Farver and Yund (1996) activation energy varies because of a change in diffusion mechanism, extrapolation of the data by 100 °C yields diffusion coefficients only about one order of magnitude lower than those measured in this study. The experimental procedures and analytical methods used in both studies are similar and the  $\text{CO}_2$  pressures were nominally the same. The technique used by Farver and Yund (1996) for creating the diffusion couple is different from that used in this study, but the difference (wet vs. dry deposition of the film) would favor enhanced diffusion rates and would suggest a greater discrepancy between data sets. A possibly more significant reason for the difference in Ca data can be found in the minor element content of the calcite samples. Farver and Yund (1996) report a uniform Mn content of about 100 ppm (100/10<sup>6</sup> Ca), whereas the calcite samples from this study contain ~500 ppm Mn and ~0.25 wt% Mg. It is known from the experiments of Kronenberg et al. (1984) that the point defects controlling electrical neutrality of the calcite structure are likely to include either singly or doubly charged Mn substitutions in the Ca sites. At least some of the difference in the diffusion results may therefore be related to variations in Mn content and its ultimate role in controlling the defect structure of calcite. It should be noted that Farver and Yund (1996) measured a different cleavage surface [the (101) surface] but also determined no measurable anisotropy in Ca diffusion based on additional measurements for surfaces parallel to the  $c$ -axis.

Fisler et al. (unpublished manuscript) recently developed a shell model to describe the bulk and defect structure of the

rhombohedral carbonate phases. The role of intrinsic  $\text{Ca}^{2+}$ - $\text{CO}_3^{2-}$  vacancy pairs in calcite was questioned due to the calculation of extremely high formation energies for the isolated defect. In contrast, substitutional defects on the Ca lattice site (e.g., Mn, Mg, Fe, and Cd) would form spontaneously and will energetically favor a different diffusion mechanism. It is quite probable that extrinsic defects, in particular those associated with multivalent Mn and Fe substitutions, will control the number of metal vacancies in calcite.

The experimental diffusion coefficients obtained in this study can be applied directly to the evaluation of several diffusion-controlled processes in carbonate minerals. Deformation in coarse-grained polycrystalline rocks such as limestone is commonly controlled by the lattice diffusion of the slowest intrinsic species. The present results indicate that at lower temperatures (down to 550 °C), Ca remains the slowest diffusing species in calcite and is rate-controlling for deformation processes at these conditions. Additionally, the homogenization of carbonate phases and the concept of closure temperature can be addressed with regard to the experimental diffusion values and Arrhenius parameters. Figure 7 illustrates the general relationship among temperature, cooling rate, and grain size based on the Dodson (1973) model for closure temperature. The closure temperature calculations imply that for very fine-grained (<1  $\mu\text{m}$ ) carbonate phases, inhomogeneous assemblages will be retained at temperatures below 300–400 °C for geologically reasonable cooling rates. The analysis using the Dodson model is a fairly broad treatment in which the total homogenization rate of a mineral grain is accomplished by diffusive transport.

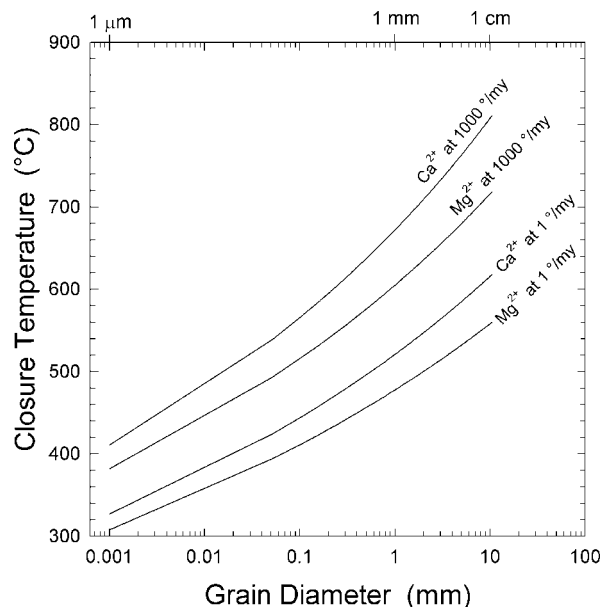


**FIGURE 7.** Closure temperature as a function of grain diameter (and cooling rate) showing the maximum temperatures required to homogenize a heterogeneous carbonate assemblage by diffusion of cations based on the experimental Arrhenius values for Ca and Mg diffusion.

A significant implication of the diffusion rate data is related to the preservation of calcite and dolomite compositions needed in geothermometry of metamorphic rocks (Anovitz and Essene 1987; Letargo et al. 1995). The Dodson model, as presented in Figure 7 for the calcite diffusion data, suggests that in regional metamorphic terrains, where cooling rates are on the order of 1 °/m.y., the compositions and corresponding temperatures associated with the calcite-dolomite geothermometer will not be preserved except at temperatures above 500 °C (for a 1 mm grain). In contrast, contact metamorphic terrains, where cooling rates are on the order of 1000 °/m.y., will most likely have the calcite-dolomite compositions preserved and not reset by chemical diffusion. Cook and Bowman (1994) and Ferry (1996) provide recent examples of the application of the calcite-dolomite geothermometer to contact aureoles and discuss the appropriateness of the derived temperatures.

The application of the calcite diffusion in the analysis of the ALH84001 meteorite is provided by Fisler and Cygan (1998). The experimental diffusion data were used to determine the conditions required for the preservation of zoned carbonate globules and to model the cooling history of the Martian meteorite.

A final example of the application of the experimental diffusion data is dolomitization. The dolomitization of limestones is a geological process that occurs globally and has been suggested to be controlled by a lattice diffusion process (Hardie 1987). The calculations of Bratter et al. (1972) have shown that if dolomitization occurs by cation replacement under dry conditions and if transport occurs by a diffusion mechanism, the naturally observed alteration rates of hundreds of angstroms per thousand years would require a diffusion coefficient of approximately  $10^{-24}$  m<sup>2</sup>/s. Extrapolating the experimental Mg diffusion rates for calcite to 30 °C, by assuming a constant diffusion mechanism, yields a diffusion rate of approximately  $10^{-53}$  m<sup>2</sup>/s. Assuming there is not a dramatic change in the mechanism for lattice diffusion below 500 °C, cation diffusion remains an unlikely process for controlling the dolomitization of limestone. More plausible mechanisms involve solution and precipitation or possibly the mechanical disruption of the carbonate lattice for the ingress of  $\text{Mg}^{2+}$  into the calcite.

## ACKNOWLEDGMENTS

We are thankful for the thorough reviews provided by Daniele Cherniak and Ted Lobotka. Their comments and suggestions added greatly to the content of the final paper. Reviews by Hank Westrich and Jim Krumhansl on an early draft of the manuscript were also very helpful. This research was supported by the U.S. Department of Energy, Office of Basic Energy Science, Geoscience Research, under contract DE-AC04-94AL85000 with Sandia National Laboratories.

## REFERENCES CITED

- Anderson, T.F. (1969) Self-diffusion of carbon and oxygen in calcite by isotope exchange with carbon dioxide. *Journal of Geophysical Research*, 74, 3918–3932.
- Anovitz, L.M. and Essene, E.J. (1987) Phase equilibria in the system  $\text{CaCO}_3$ - $\text{MgCO}_3$ - $\text{FeCO}_3$ . *Journal of Petrology*, 28, 389–414.
- Brady, J.B. and McCallister, R.H. (1983) Diffusion data for clinopyroxenes from homogenization and self-diffusion experiments. *American Mineralogist*, 68, 95–105.
- Bratter, P., Moller, P., and Rosnick, U. (1972) On the equilibrium of coexisting sedimentary carbonates. *Earth and Planetary Science Letters*, 14, 50–54.
- Cherniak, D. (1997) An experimental study of strontium and lead diffusion in calcite, and implications for carbonate diagenesis and metamorphism. *Geochimica*

- et *Cosmochimica Acta*, 61, 4173–4179.
- (1998) REE diffusion in calcite. *Earth and Planetary Science Letters*, 160, 273–287.
- Cook, S.J. and Bowman, J.R. (1994) Contact-metamorphism surrounding the Alta stock: Thermal constraints and evidence of advective heat-transport from calcite + dolomite geothermometry. *American Mineralogist*, 79, 513–525.
- Crank, J. (1975) *The mathematics of diffusion* (2nd edition), 414 p., Oxford University Press, London.
- Dodson, M.H. (1973) Closure temperature in cooling geochronological and petrological systems. *Contributions to Mineralogy and Petrology*, 40, 259–274.
- Elphick, S.C., Ganguly, J., and Loomis, T.P. (1985) Experimental determination of cation diffusivities in aluminosilicate garnets: 1. Experimental methods and interdiffusion data. *Contributions to Mineralogy and Petrology*, 90, 36–44.
- Farver, J.R. and Yund, R.A. (1996) Volume and grain boundary diffusion of calcium in natural and hot-pressed calcite aggregates. *Contributions to Mineralogy and Petrology*, 123, 77–91.
- Ferry, J.M. (1996) 3 novel isograds in metamorphosed siliceous dolomites from the Ballachulish aureole, Scotland. *American Mineralogist*, 81, 485–494.
- Fisler, D.K. and Cygan, R.T. (1998) Constraints on the thermal history of ALH84001 from calcite diffusion experiments. *Meteoritics and Planetary Science*, 33, 785–790.
- Ganguly, J., Tirone, M., and Hervig, R.L. (1998) Diffusion kinetics of samarium and neodymium in garnet, and a method for determining cooling rates of rocks. *Science*, 281, 805–807.
- Goldsmith, J.R. (1959) Some aspects of the geochemistry of carbonates. In P.H. Abelson, Ed., *Researches in geochemistry*, Wiley, New York.
- Hardie, L.A. (1987) Perspectives: Dolomitization: A critical view of some current views. *Journal of Sedimentary Petrology*, 57, 166–183.
- Haul, R.A.W. and Stein, L.H. (1955) Diffusion in calcite crystals on the basis of isotopic exchange with carbon dioxide. *Transactions of the Faraday Society*, 51, 1280–1290.
- Kronenberg, A.K., Yund, A.R., and Gilletti, B.J. (1984) Carbon and oxygen diffusion in calcite: Effects of Mn content and  $P_{H_2O}$ . *Physics and Chemistry of Minerals*, 11, 101–112.
- Letargo, C.M.R., Lamb, W.M., and Park, J.S. (1995) Comparison of calcite + dolomite thermometry and carbonate + silicate equilibria: Constraints on the condition of metamorphism of the Llano uplift, central Texas, U.S.A. *American Mineralogist*, 80, 131–143.
- Mirwald, P.W. (1976) A differential thermal analysis study of the high-temperature polymorphism of calcite at high pressures. *Contributions to Mineralogy and Petrology*, 59, 33–44.
- (1979a) Determination of a high-temperature transition of calcite at 800°C and one bar  $CO_2$  pressure. *Neues Jahrbuch für Mineralogie*, 7, 309–315.
- (1979b) Electrical conductivity of calcite between 300 and 1200°C at a  $CO_2$  pressure of 40 bars. *Physics and Chemistry of Minerals*, 4, 291–297.
- Paulin, L. (1960) *The nature of the chemical bond* (3rd edition), 644 p., Cornell University Press, Ithaca, New York.
- Reeder, R.J. and Grams, J.C. (1987) Sector zoning in calcite cement crystals: Implications for trace-element distributions in carbonates. *Geochimica et Cosmochimica Acta*, 51, 187–194.
- Romanek, C.S., Grady, M.M., Wright, I.P., Mittlefehldt, D.W., Socki, R.A., Pillinger, C.T., and Gibson, E.K. (1994) Record of fluid-rock interactions on Mars from the meteorite ALH84001. *Nature*, 372, 655–657.
- Ryerson, F.J., Durham, W.B., Cherniak, D.J., and Lanford, W.A. (1989) Oxygen diffusion in olivine: Effect of oxygen fugacity and implications for creep. *Journal of Geophysical Research*, 94, 4105–4118.
- Schwandt, C.S., Cygan, R.T., and Westrich, H.R. (1993) A thin film approach for producing diffusion couples. *Pure and Applied Geophysics*, 103, 631–642.
- (1998) Magnesium self-diffusion in orthoenstatite. *Contributions to Mineralogy and Petrology*, 130, 390–396.

MANUSCRIPT RECEIVED JUNE 22, 1998

MANUSCRIPT ACCEPTED APRIL 26, 1999

PAPER HANDLED BY PETER I. NABELEK